Fine structure of the electron paramagnetic resonance spectrum of Fe^{3+} centres in $LiTaO_3$

Fine structure of the electron paramagnetic resonance spectrum of Fe^{3+} centres in $LiTaO_3$

V A Vazhenin[1], **V B Guseva**[1], **M Yu Artyomov**[1], **R K Route**[2], **M M Fejer**[2] **and R L Byer**[2]

[1] Institute of Physics and Applied Mathematics, Ural State University, Ekaterinburg 620083, Russia
[2] E L Ginzton Laboratory, Stanford University, Stanford, CA 94305, USA

Abstract

The electron paramagnetic resonance spectrum of trigonal Fe^{3+} centres has been investigated and parameters of the spin Hamiltonian obtained for nominally pure congruent $LiTaO_3$ crystals annealed at ~1500 K under Li_2O vapour pressure corresponding to the pressure over the stoichiometric lithium tantalate. The possibility of calculating the zero-field splitting of the ground state of the impurity ion on the basis of the superposition model is discussed.

1. Introduction

The practically important electro-optical parameters of ferroelectric $LiNbO_3$ and $LiTaO_3$ single crystals (having identical structure and similar properties) depend on the methods of growth and further processing of the crystals, which can significantly change the degree of crystal perfection. Important information about the nature and concentration of defects, both paramagnetic ones and those compensating for the extra charge of the former, in the crystals mentioned can be obtained by magnetic resonance methods. Ions of elements belonging to the iron group are good paramagnetic probes for studies of this kind. Furthermore, it is known that iron impurity ions in lithium tantalate and lithium niobate play a key role in the photorefractive effect.

The electron paramagnetic resonance (EPR) and the electron–nuclear double resonance (ENDOR) of trigonal Fe^{3+} centres in a doped (0.01 at.%) congruent $LiTaO_3$ crystal were investigated in [1]. Because of the large linewidth and the non-canonical line-shape leading to a large uncertainty in determining the positions of lines, it was found sufficient to use just two parameters for describing the observed EPR spectrum: the isotropic g-factor and the axial fine-structure parameter $b_{20} = 3302 \times 10^{-4}$ $cm^{-1} = 9900$ MHz. An ENDOR data analysis [1] furnished conclusive evidence that the Fe^{3+} ion is localized in lithium tantalate at the Li^+ site with symmetry C_3. The large linewidth and unusual shape of the EPR lines are presumably due to the very high concentration of defects (Li^+ vacancies), at which virtually any paramagnetic ion has in its environment a charged defect giving rise to off-diagonal parameters
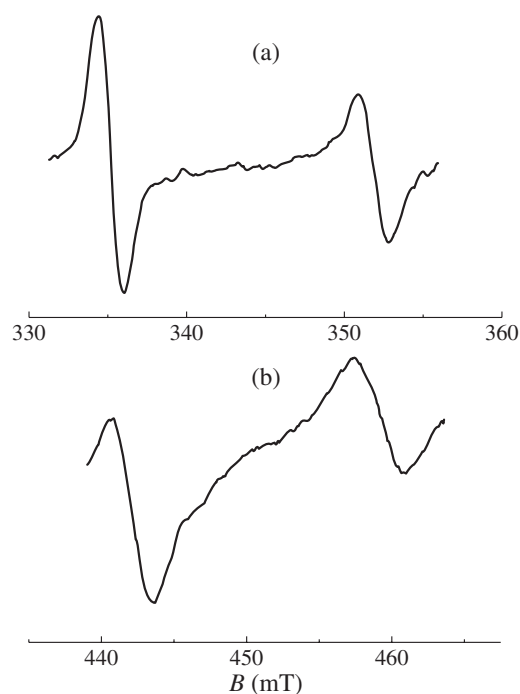
Figure 1. The EPR spectrum of Fe^{3+} centres in $LiTaO_3$ at room temperature. (a) The transitions $-1/2 \leftrightarrow +1/2$ and $-3/2 \leftrightarrow -1/2$ at $B \parallel C_3$; (b) the doublet splitting of the high-field transition $-3/2 \leftrightarrow +1/2$; polar angle $\theta = 30°$, azimuth angle $\varphi = 0$.

of the spin Hamiltonian, noticeable in the EPR. This means that the spectrum observed is a superposition of spectra with trigonal, monoclinic, and triclinic symmetry.

The aim of the present study was to analyse the EPR of trigonal Fe^{3+} centres in $LiTaO_3$ and to compare the results obtained with those furnished by the superposition model for zero-field splitting of the ground state.

2. Experimental procedure and results

Nominally pure congruent $LiTaO_3$ single crystals were studied. The crystals were subjected to prolonged (hundreds of hours) high-temperature ($\sim$1500 K) annealing in the presence of a mixture of Li_2O and Ta_2O_5, which ensured a Li_2O vapour pressure exactly corresponding to the Li_2O vapour pressure over the stoichiometric lithium tantalate at the given temperature [2, 3].

The samples were in the form of $\sim$0.5 mm thick single-crystal polished wafers of area 1 cm^2, cut out perpendicularly to the optical axis. The measurements were carried out at room temperature on an EPR spectrometer with magnetic field modulation and a cylindrical microwave cavity of the type H_{011} (9.38 GHz). For all of the crystals mentioned above, the EPR spectrum of the trigonal Fe^{3+} centre was characterized by zero-field splitting close to that measured in [1] and symmetrical signals (without indications of superfine structure) with linewidths at $B \parallel C_3$ (B is the magnetic field induction) of about 2 mT (figure 1). Judging from the spectrum intensity, the iron content does not exceed 10^{-4} at.%. The iron present in the crystals studied presumably originates from an uncontrollable admixture of iron in the stock used to grow the single crystals studied.
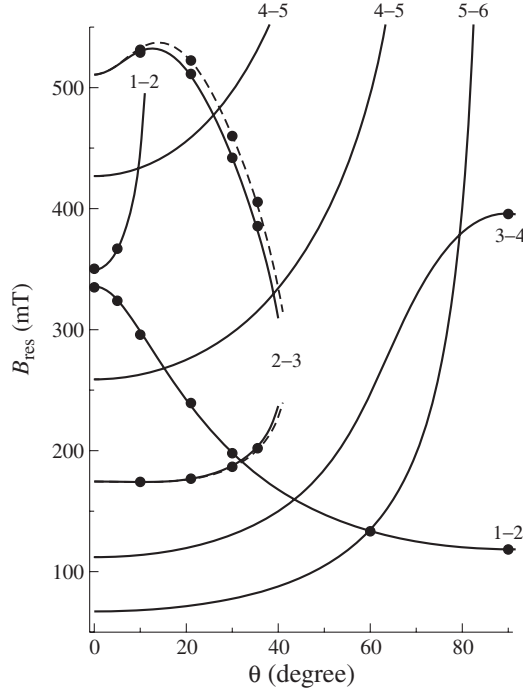
Figure 2. The polar angular dependence (zx-plane) of the resonance positions of EPR signals from Fe^{3+} centres in LiTaO$_3$. Points: experiment. $T = 305$ K, $\nu_{EPR} = 9.38$ GHz. Full and dotted curves: calculations (with the parameters given in the text) for two positions connected by reflection. The states are numbered from bottom to top.

In an arbitrarily oriented magnetic field, a doublet splitting of the spectrum is observed (figure 1(b)). In contrast to the case of EPR in ferroelectric germanates of lead (Gd^{3+}) [4] and lithium (Mn^{2+}) [5], this splitting does not result from the presence of two types of domain, but is due to the existence in the structure of the LiTaO$_3$ ferroelectric phase of two Li$^+$ (and also Ta^{5+}) positions with symmetry C_3, connected by the σ_v-operation. In the ($z \parallel C_3, x \perp \sigma_v$) coordinate system, the spin Hamiltonians of these two centres differ solely in the sign of the b_{43}-parameter. The angular behaviour of the resonance magnetic fields at 305 K in the coordinate system mentioned above is characterized by the spin Hamiltonian [6] (figure 2)

$$H = g\beta B \cdot S + \tfrac{1}{3}b_{20}O_{20} + \tfrac{1}{60}(b_{40}O_{40} + b_{43}O_{43}) \tag{1}$$

where g is the g-tensor, β is the Bohr magneton, S is the spin moment, and O_{nm} are the Stevens spin operators with the parameters $g_\parallel = 2.001(1)$, $g_\perp = 1.998(15)$, $b_{20} = 9600(20)$ MHz, $b_{40} = 5(5)$ MHz, $b_{43} = \pm 4180(25)$ MHz on the assumption of positive b_{20}.

With increasing temperature, the $-1/2 \leftrightarrow -3/2$ transition ($B \parallel C_3$) shifts in the direction of the $-1/2 \leftrightarrow 1/2$ transition. At $T \approx 380$ K they merge as a result of the accidental crossing of the energy levels with $m_s + 1/2$ and $-3/2$. In contrast to the case for Fe^{3+} centres in congruent crystals not subjected to the annealing procedure described above, the absence of shape distortions for this transition near the coincidence of their positions indicates that the fine-structure parameters of the b_{n2} type are close to zero.

Table 1. Spherical coordinates of nearest-neighbour oxygen ions for Li^+ and Ta^{5+} in $LiTaO_3$ [7].

	Li	Ta
R_1 (nm)	0.231 10	0.190 82
θ_1 (deg)	42.87	60.25
R_2 (nm)	0.204 55	0.207 40
θ_2 (deg)	107.15	130.61

3. Discussion

In [7], the fine-structure parameters characterizing the EPR spectrum of the Fe^{3+} ion in lithium tantalate were calculated using the Newman superposition model [8], which assumes that the contributions from ligands are additive:

$$b_{nm} = \sum_i K_{nm}(\theta_i \varphi_i) \bar{b}_n(R_0) \left(\frac{R_0}{R_i} \right)^{t_n} \tag{2}$$

where t_n, $\bar{b}_n(R_0)$ are the intrinsic parameters of the model, and $K_{nm}(\theta_i, \varphi_i)$ is the 'coordination factor', for the cases of Fe^{3+} localization at Li^+, Ta^{5+} and structural vacancy sites (point symmetry group C_3). For the second-rank parameter b_{20} at the Li^+ site, the following values were obtained: 11 680, 10 615, and 11 131 MHz, differing in the choice of parameters of the model employed. For example, the first value corresponds to a set of intrinsic parameters obtained in uniaxial-stress experiments with MgO [9]. The fact that these values are close to the experimental value (9900 MHz) led to the conclusion that the Li^+ ion is replaced by Fe^{3+}, in agreement with [1]. It should be noted that the calculations used the structural parameters of impurity-free $LiTaO_3$ (table 1).

The superposition approximation with model parameters $\bar{b}_4(R_0) = 87$ MHz, $R_0 = 0.21$ nm, and $t_4 = 14$ characteristic of Fe^{3+} in MgO was used in [7] to obtain, in addition to the axial parameter b_{20}, the fourth-rank constants $b_{40} = 8.7$ MHz and $b_{43} = 6461$ MHz. It can be seen that these values are in good agreement with the results of the present study as regards both the order of magnitude and the sign.

In the authors' opinion, it is of interest to consider the behaviour of the parameter b_{40} for high-symmetry Fe^{3+} centres for a wider set of materials. Figure 3 presents experimental values of the fine-structure parameter b_{40} ($z \parallel C_4$) for undistorted octahedral Fe^{3+} complexes in relation to the distance to the nearest anions in a lattice undisturbed by impurity ions. In view of the fact that the nearest environment of a Li^+ site in lithium tantalate is a rather strongly distorted octahedron (with distances to ligands of 0.231 and 0.205 nm [7]), placing data on b_{40} for $LiTaO_3:Fe^{3+}$ in figure 3 would be incorrect. The curve connecting the points for CaO and MgO in figure 3 represents the result obtained using formula (2) with the parameters $\bar{b}_4(R_0) = 88$ MHz, $R_0 = 0.21$ nm, $t_4 = 8.7$ and cannot describe adequately the real radial dependence of b_{40} if only because that relaxation of the dimensions of the octahedral complex would be expected, because of the introduction of an impurity. However, it is apparent, in the authors' opinion, that allowing reasonable changes in distances to ligands fails to account for the deviation of b_{40} in crystals with perovskite-type structure from the curve obtained.

Since all the perovskite crystals whose parameters are presented in figure 3 exhibit structural transitions, it is appropriate to recall that, in addition to the static contribution to the parameters of the spin Hamiltonian, which takes into account the cluster geometry [8], there exists a dynamic contribution associated with the spin–phonon coupling [15]. It was shown in [16] that, for crystals with structural transitions, the dynamic contribution to the ground-state splitting includes, in addition to Debye's term, a term that is related to the interaction
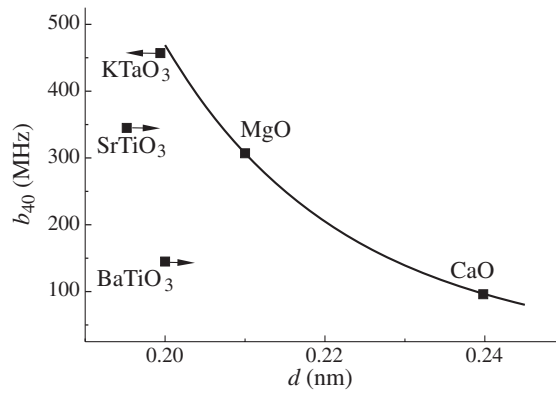
Figure 3. The dependence of the b_{40}-parameter of cubic Fe^{3+} centres on the distance to ligands in the undistorted lattice [10–14]. The measurements were at 77 K for CaO, 410 K for BaTiO$_3$, and room temperature for the rest of the cases. The arrows show the most likely directions of d-relaxation upon doping.

with the soft-phonon mode and, therefore, demonstrates a singularity near the phase transition temperature T_c:

$$b_{40} \sim \frac{1}{d^t}\left[1 + \frac{t(t+1)kT}{4}\left(f_1 + f_2\frac{C}{|T - T_c|}\right)\right] \tag{3}$$

where d is the distance to the ligands, k is Boltzmann's constant, C is the Curie constant, f_1 and f_2 are dimensional positive coefficients reflecting the influence of a phonon on the distance to the ligands, and parameter t is analogous to t_4 in expression (2). This term may lead to an appreciable modification of b_{40}, at least near T_c. However, the constant sign of the dynamic contributions gives no way of understanding, at least qualitatively, the scatter of the points in figure 3.

The applicability of the superposition approach was substantiated in [17, 18] for the second-rank ground-state-splitting parameters of rare-earth ions Gd^{3+} and Eu^{2+}. Also, a modification of expression (2) was proposed. For ions of iron group elements, no substantiation of this kind can be found in the literature, especially for fourth-rank fine-structure parameters. In [19], fourth-rank intrinsic parameters were given for Gd^{3+} centres with sixfold, eightfold and twelvefold coordinations. These data show strong scatter, to the point of a change of the sign of $\bar{b}_4(R_0)$ on going to compounds of different structures. The instability of t_4 for octahedral Fe^{3+} centres in crystals with MgO structure is also indicated by the significant modification of its value (see above) on taking into account data for the isostructural CaO crystal. Therefore, the model [8] gives us reason to believe that the intrinsic parameters are, at best, constant within a set of isostructural crystals.

Returning to figure 3, it can be noted that, in perovskite crystals, the Fe^{3+} ion with the ionic radius of 0.064 nm substitutes for Ta^{5+} (0.068 nm) and Ti^{4+} (0.0605 nm) ions. Taking account of this fact, the most probable direction of relaxation of distances to the ligands upon introduction of an impurity is shown in figure 3 by arrows. A curve can be drawn through the new positions of the points, which describes a strong, but smooth dependence on distance, based on intrinsic parameters of the superposition model under discussion for b_{40} for octahedral Fe^{3+} centres in oxide perovskites.

And, finally, since the structure of LiTaO$_3$ differs significantly from that of MgO, the good agreement between the calculated [7] and experimental fourth-rank fine-structure parameters

of the EPR spectrum of Fe^{3+} in lithium tantalate may just be a happy coincidence. This conclusion in no way casts doubt on the finding [1] that Fe^{3+} is localized in $LiTaO_3$.

4. Conclusions

It was found that high-temperature annealing of congruent $LiTaO_3$ single crystals under Li_2O vapour pressure corresponding to the pressure over the stoichiometric lithium tantalate substantially lowers the defect concentration that can be detected by means of the paramagnetic resonance.

This made it possible to determine all fine-structure parameters of trigonal Fe^{3+} centres in $LiTaO_3$, which proved to be close to those calculated by Yeom in the superposition approximation.

An analysis of published data on the zero-field splitting for the Fe^{3+} centres in the octahedral oxygen environment demonstrated that such good coincidence of the experimental and calculated fourth-rank parameters in $LiTaO_3:Fe^{3+}$ may be accidental.

Acknowledgment

References

[1] Söthe H, Rowan L G and Spaeth J-M 1989 *J. Phys.: Condens. Matter* **1** 3591
[2] Shur V Ya, Blankova E B, Rumyantsev E L, Nikolaeva E V, Shishkin E I, Barannikov A V, Route R K, Fejer M M and Byer R L 2002 *Appl. Phys. Lett.* **80** 1
[3] Bordui P, Norwood R, Jundt D and Fejer M 1992 *J. Appl. Phys.* **71** 875
[4] Vazhenin V A, Guseva V B, Shur V Ya, Nikolaeva E V and Artemov M Yu 2001 *Phys. Solid State* **43** 1952
[5] Trubitsyn M P 1998 *Phys. Solid State* **40** 101
[6] Al'tshuler S A and Kozyrev B M 1974 *EPR in Compounds of Transition Elements* (New York: Wiley)
[7] Yeom T H 2001 *J. Phys.: Condens. Matter* **13** 10471
[8] Newman D J and Urban W 1975 *Adv. Phys.* **24** 793
[9] Siegel E and Müller K A 1979 *Phys. Rev.* B **19** 109
[10] Low W 1956 *Proc. Phys. Soc.* B **69** 1169
[11] Shuskus A J 1962 *Phys. Rev.* **127** 1529
[12] Müller K A 1958 *Helv. Phys. Acta* **31** 173
[13] Hannon D M 1967 *Phys. Rev.* **164** 366
[14] Sakudo T 1963 *J. Phys. Soc. Japan* **18** 1626
[15] Walsh W M, Jeener J and Bloembergen N 1965 *Phys. Rev.* **139** A1338
[16] Rytz D, Höchli U T, Müller K A, Berlinger W and Boatner L A 1982 *J. Phys. C: Solid State Phys.* **15** 3371
[17] Levin L I 1986 *Phys. Status Solidi* b **134** 275
[18] Levin L I and Gorlov A D 1992 *J. Phys.: Condens. Matter* **4** 1981
[19] Arakawa M, Aoki H, Takeuchi H, Yosida T and Horai K 1982 *J. Phys. Soc. Japan* **51** 2459